Multifunctional $BiFeO_3/TiO_2$ nano-heterostructure: Photo-ferroelectricity, rectifying transport, and nonvolatile resistive switching property

Ayan Sarkar, Gobinda Gopal Khan' , Arka Chaudhuri, Avishek Das, and Kalyan Mandal

Citation: Appl. Phys. Lett. **108**, 033112 (2016); doi: 10.1063/1.4940118
View online: http://dx.doi.org/10.1063/1.4940118
View Table of Contents: http://aip.scitation.org/toc/apl/108/3
Published by the American Institute of Physics

Multifunctional $BiFeO_3/TiO_2$ nano-heterostructure: Photo-ferroelectricity, rectifying transport, and nonvolatile resistive switching property

Ayan Sarkar,[1] Gobinda Gopal Khan,[1,a)] Arka Chaudhuri,[2,3] Avishek Das,[4] and Kalyan Mandal[2]
[1]*Centre for Research in Nanoscience and Nanotechnology, University of Calcutta, Technology Campus, Block JD2, Sector III, Salt Lake City, Kolkata 700 098, India*
[2]*Department of Condensed Matter Physics and Material Sciences, S. N. Bose National Centre for Basic Sciences, Block JD, Sector III, Salt Lake City, Kolkata 700 098, India*
[3]*Department of Applied Science, Haldia Institute of Technology, Haldia 721657, Purba Medinipur, West Bengal, India*
[4]*Department of Electronic Science, University of Calcutta, 92 APC Road, Kolkata 700009, India*

(Received 14 August 2015; accepted 6 January 2016; published online 21 January 2016)

Multifunctional $BiFeO_3$ nanostructure anchored TiO_2 nanotubes are fabricated by coupling wet chemical and electrochemical routes. $BiFeO_3/TiO_2$ nano-heterostructure exhibits white-light-induced ferroelectricity at room temperature. Studies reveal that the photogenerated electrons trapped at the domain/grain boundaries tune the ferroelectric polarization in $BiFeO_3$ nanostructures. The photon controlled saturation and remnant polarization opens up the possibility to design ferroelectric devices based on $BiFeO_3$. The nano-heterostructure also exhibits substantial photovoltaic effect and rectifying characteristics. Photovoltaic property is found to be correlated with the ferroelectric polarization. Furthermore, the nonvolatile resistive switching in $BiFeO_3/TiO_2$ nano-heterostructure has been studied, which demonstrates that the observed resistive switching is most likely caused by the electric-field-induced carrier injection/migration and trapping/detrapping process at the hetero-interfaces. Therefore, $BiFeO_3/TiO_2$ nano-heterostructure coupled with logic, photovoltaics and memory characteristics holds promises for long-term technological applications in nanoelectronics devices. © *2016 AIP Publishing LLC*. [http://dx.doi.org/10.1063/1.4940118]

Multiferroic oxides hold immense potential for multifunctional applications in data storage, random access memory, spintronics, filters, attenuators, sensors, and photovoltaic devices because of their fundamental physical properties.[1–6] Among multiferroic oxides, bismuth ferrite ($BiFeO_3$) has earned ever-increasing attraction because of its coupling of ferroelectricity and magnetism, promising for magnetoelectric device fabrication.[4] Along with this, recently, various interesting physical properties of $BiFeO_3$, such as photovoltaic and photo-ferroelectric effects under visible light,[5–7] spontaneous polarization,[4] piezoelectric effect,[8] switchable ferroelectric diode characteristics,[9] resistive switching (RS),[10,11] and magnetoelectric behaviour,[4] have been investigated considering its promises to meet the aspirations for the next generation multifunctional devices. However, in many situations, the issues like crystallinity, leakage property, and volatile nature of bismuth are found to affect negatively on the performance of $BiFeO_3$.[12–14] In this concern, several strategies have been developed by the researchers to improve the multifunctionality of $BiFeO_3$.[10,12–14] Moreover, $BiFeO_3$ has been studied well mostly in its bulk and thin films although $BiFeO_3$ nanostructures should have quite interesting properties arising because of the morphology and the quantum size effects. In fact $BiFeO_3$ in the form of nanostructures has not been studied well enough in the area related to solid state electronics.

This work reports an efficient approach to achieve multifunctionality in $BiFeO_3$ nanostructures grown on wide band gap TiO_2 nanotubes (NTs) substrate (see supplementary material).[15,16] TiO_2 NTs serve as the insulating oxide mask having large surface area where the interfacial interaction between $BiFeO_3/TiO_2$ nano-heterojunctions provide opportunity to achieve significant multifunctionality. $BiFeO_3$ nanostructures are found to exhibit stable ferroelectric behaviour, in comparison to that of the pure $BiFeO_3$ NTs reported in our previous work.[17] Most interestingly, we have observed the white-light-induced ferroelectricity in $BiFeO_3$ nanostructures. The coupling of visible light and ferroelectricity in $BiFeO_3$ nanostructures has not been studied till to date. The demonstration on the origin of the photon induced ferroelectricity not only provides insights of the physical property but also boosts the opportunity to design light-controlled switchable ferroelectric devices based on $BiFeO_3$. The same nanostructure also exhibits ferroelectric diode like rectifying characteristics and photovoltaic effect. Furthermore, the resistive switching behaviour of the $BiFeO_3/TiO_2$ nano-heterostructure has been found to be interesting where the electronic conduction could be easily switched between nonvolatile "ON" (low resistance state, LRS) and "OFF" (high resistance states, HRS) states with applied external bias. This phenomenon holds immense promise for the application in semiconductor based nonvolatile resistance random access memory (ReRAM) devices. Therefore, the light controlled ferroelectricity, photovoltaic, and rectifying properties coupled with the resistive switching behaviour in $BiFeO_3/TiO_2$ nano-heterostructure open up the opportunity to fabricate $BiFeO_3$ based multifunctional nanoelectronics devices.

The morphology and structure of the as prepared $BiFeO_3/TiO_2$ nano-heterostructure, examined by the field emission scanning electron microscope (FESEM, JEOL JSM-7600F) show vertically aligned uniform nano tubular arrays of diameters ~120 nm (Figure 1(a)). The transmission electron

a)Author to whom correspondence should be addressed. Electronic mail: gobinda.gk@gmail.com

microscope (HRTEM, JEOL JEM-2100) studies show the well covered wrapping of the particle like $BiFeO_3$ nanostructures on the surface of TiO_2 NTs (Figures 1(b)–1(d)), whereas the high resolution TEM micrograph (Figure 1(e)) indicates some superimposed $BiFeO_3$ nanostructures having the dimension ~15–20 nm on the TiO_2 NT's body. The x-ray diffraction (XRD, Panalytical X'Pert Pro diffractometer) patterns for both pristine TiO_2 NTs and $BiFeO_3/TiO_2$ nano-heterostructure have been recorded using Cu K_α line ($\lambda = 1.54$ Å). The XRD pattern (Figure 1(f)) demonstrates that $BiFeO_3$ is polycrystalline, single phase material that corresponds to the rhombohedral distorted perovskite structure of $BiFeO_3$ with $R3c$ space group (JCPDS File#20-0169) (see supplementary material).[15] The elemental colour mappings (Figures 1(h)–1(k)) performed by using energy dispersive x-ray spectroscopy (EDS, Oxford Instruments, attached to the FESEM) confirm the homogeneous distribution of the Ti, Bi, Fe, and O on the surface of $BiFeO_3/TiO_2$ nano-heterostructure.

Figure 2(a) shows the room temperature (RT) *P-E* hysteresis loops for the $BiFeO_3$ nanostructures anchored on TiO_2 NTs under dark and visible white light illumination (10 mW/cm^2) conditions with various voltages with the applied magnetic field of $H = 0$. Inset of Figure 2(a) shows the schematic diagram of the experimental setup used for the ferroelectric hysteresis loop measurements, where the $BiFeO_3$ nanostructures are anchored on the insulating TiO_2 NTs surface and Ag and Ti (substrate underneath) act as two electrodes. The variation of the ferroelectric polarization under dark and light irradiation conditions for the applied voltages of 30 and 300 V are shown in Figure 2(b). *P-E* hysteresis loops for the $BiFeO_3$ nanostructures at different applied voltages under dark and light-illumination conditions are shown in Figure S6 in the supplementary material.[15] Clear evidence of ferroelectricity is found for the $BiFeO_3$ nanostructures where the hysteresis could be related with the ferroelectric polarization. It is to be mentioned that the pristine TiO_2 NTs exhibit no ferroelectric signature. The stable electrical polarization with saturation ferroelectric polarization for the $BiFeO_3$ nanostructures is found to be improved than that of the $BiFeO_3$ NTs reported in our previous work,[17] where the $BiFeO_3$ nanotube samples exhibited no hysteresis or lossy type hysteresis characteristics (pristine $BiFeO_3$ and doped $BiFeO_3$ nanotubes samples measured with both ends having Ag electrodes). Therefore, it is believed that the insulating TiO_2 NTs not only act as the mask for the growth of $BiFeO_3$ nanostructures but also provide the platform to reduce the leakage current problem and hence stable and enhanced ferroelectric polarization in $BiFeO_3$ nanostructure is obtained.[9,18] However, the unsaturated nature of the *P-E* loops might indicate that the ferroelectricity is because of the resistivity of the structures. Most interestingly, here we have observed a distinctive photo-ferroelectric effect in $BiFeO_3$ nanostructures. The saturation ferroelectric polarization and the remnant ferroelectric polarization are found to increase instantly with the incidence of visible white light ($\lambda > 420$ nm) from an ordinary electric lamp (10 mW/cm^2). The above changes are found to be more prominent at the low applied voltage (30 V). With the increase of the applied voltage, the photo-ferroelectric effect is found to become feeble. The variations of the saturation and remnant ferroelectric polarizations with the applied voltage under dark and light-illumination conditions are summarized in Table S1 (see supplementary material).[15] Figure 2(c) shows the visible white light induced changes of saturation ferroelectric polarization (ΔP) of $BiFeO_3/TiO_2$ nano-heterostructure with respect to the applied voltage. Here, ΔP is defined as $(P_{light} - P_{dark})/P_{dark}$, where P_{dark} and P_{light}, respectively, are the saturation ferroelectric polarizations in dark and light-illumination conditions. It is evident from Figure 2(c) that with the increase of the applied voltage, ΔP decreases exponentially. With the increase of the applied voltage from 30 to 100 V, ΔP decreases sharply and then ΔP decreases steadily with the increase of the voltage beyond 100 V. ΔP decreases from 44% to 5% with the increase of the applied voltage from 30 to 300 V. The change in the remnant ferroelectric polarization (ΔP_R) with the illumination of white light with respect to the applied voltage has been plotted in Figure 2(d). Here, ΔP_R is defined as $(P_{R\ (light)} - P_{R\ (dark)})/P_{R\ (dark)}$, where $P_{R\ (dark)}$ and $P_{R\ (light)}$, respectively, are the remnant ferroelectric polarizations in dark and light-illumination conditions. It is found that ΔP_R also decreases exponentially with the increase of the voltage. Here, the change in ΔP_R is found to be consistent with the voltage. ΔP_R is about 33% at the low applied voltage of 30 V while it becomes only 11% when the voltage increases to 300 V. The instant change in the saturation and remnant

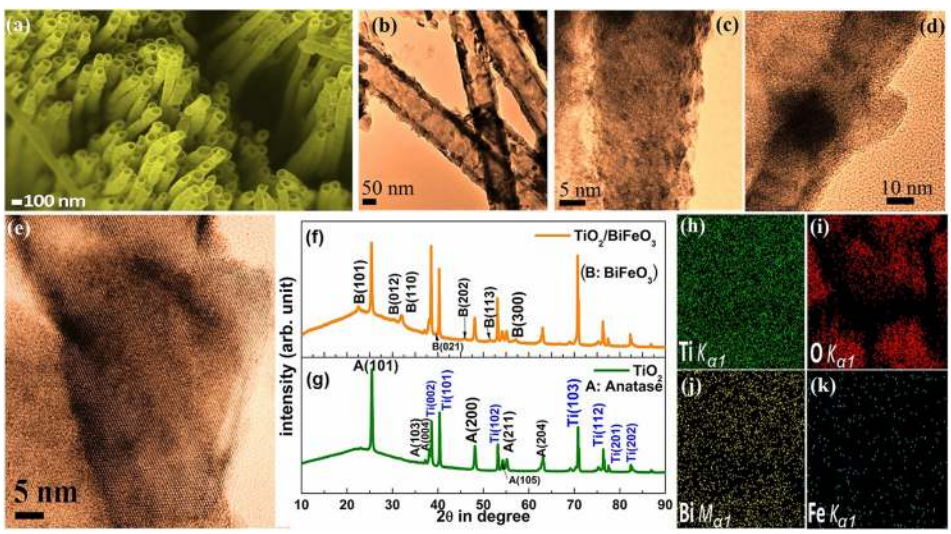

FIG. 1. FESEM (a), TEM (b)–(d), and HRTEM (e) images of the $BiFeO_3$ nanostructure anchored TiO_2 NTs. XRD patterns of the $BiFeO_3/TiO_2$ nano-heterostructure (f) and TiO_2 NTs (g). (h)–(k) EDS colour mapping of the top surface of $BiFeO_3$ $BiFeO_3/TiO_2$ nano-heterostructure.

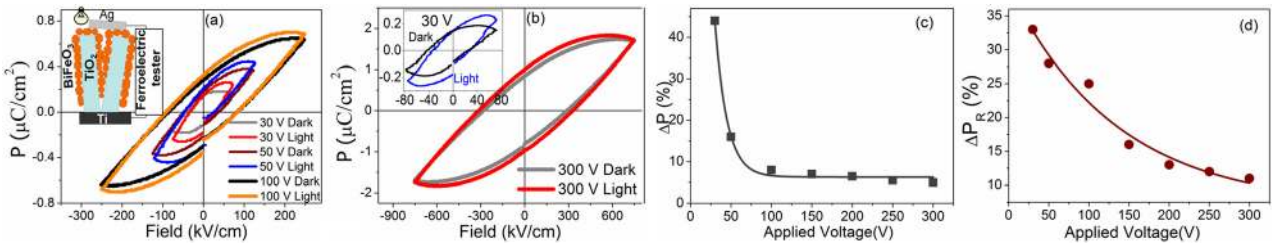

FIG. 2. (a) and (b) and the inset of (b): variations of the room temperature *P-E* hysteresis loops for the $BiFeO_3$ nanostructures anchored on TiO_2 NTs with applied voltage under dark and visible white light-illumination conditions. Inset of (a): schematic diagram of the experimental setup used for the ferroelectric hysteresis loop measurements. (c) Variation of the saturation polarization and (d) remnant polarization with applied voltage $BiFeO_3$ nanostructures on TiO_2 NTs.

polarizations with light-illumination "on" or "off" indicates that the light only triggers the ferroelectric property, where the generation of heat due to light-illumination could be overruled. This study suggests that the ferroelectric polarization in $BiFeO_3$ nanostructures can be tuned by visible light and most interestingly, the external electric field has a crucial role to control the photo-ferroelectric effect. The electric field controlled photo-ferroelectric effect in $BiFeO_3$ nanostructures helps to understand the mechanism of the photo-ferroelectric effect.

The photo-ferroelectric effect is known to physics for a long time.[19] The possible origin of the light induced change in ferroelectricity evidenced, for different materials are demonstrated based on the trapping of the photo generated charge carriers at domain/grain boundaries and the mobility of ferroelectric domains under light illumination.[22–24] The photo generation of the charge carriers in the ferroelectrics[5,6] is well known, and we also have observed the photo-generation of electrons in the $BiFeO_3$ nanostructures too (discussed later). Here, the $BiFeO_3/TiO_2$ nano-heterostructure provides large interfaces/surface area along with the grain boundaries in $BiFeO_3$ nanostructures anchored on TiO_2. Hence, the photo-generated electrons in $BiFeO_3$ nanostructures can get trapped at the interfaces and grain boundaries and induce polarization effect as evidenced for other multiferroics too.[7,20–22] Now, if the direction of polarization caused by the trapped electrons at the interfaces/grain boundaries is same as that of the $BiFeO_3$ nanostructures themselves then the resultant ferroelectric polarization of the $BiFeO_3$ nanostructures will increase with the illumination of the visible-light, as observed in this work and in case of the $BiFeO_3$ thin films, reported recently.[7] In order to get a clear idea about the mechanism of the photo-ferroelectric effect, here we have studied the effect of external electric field on the photo-ferroelectric polarization. The photo-ferroelectric effect is found to diminish remarkably with the increase of the external electric field. Hence, it is expected that the increase of the external bias will force to leave and move the trapped electrons at the interfaces/grain boundaries and therefore the population of the trapped electrons responsible for the enhancement of the ferroelectric polarization will decrease reducing the total polarization of the material. The external electric field dependent study on the photo-ferroelectric effect of $BiFeO_3$ nanostructures signifies that the enhanced photo-ferroelectric effect can be attributed to the photo-generated electrons trapped at the interfaces and grain boundaries.

The effect of visible-white light radiation on the *I-V* characteristics of $BiFeO_3$ nanostructures grown on TiO_2 NTs is shown in Figure 3. A distinct change in photoconduction is observed after light-illumination ($10\,mW/cm^2$ and $\lambda > 420\,nm$) on the $BiFeO_3$ nanostructures which also exhibits interesting photovoltaic response. The measured short-circuit current (I_{sc}) is 1 nA, and the open circuit voltage (V_{oc}) is about 0.3 V. The change in conductivity upon illumination may result because of the self-polarization of $BiFeO_3$ nanostructures[23,24] which indicates that the generation of photo-induced carriers and ferroelectric polarization is correlated to each other. The *I-V* characteristics of $BiFeO_3$ nanostructures measured in dark condition clearly demonstrate the obvious rectifying behaviour.[25–27] During a measuring cycle, the current value is switched at around ± 4 V.

Along with the ferroelectric memory characteristics, the RS property of ferroelectric oxides, where the oxide changes its internal conductivity according to the history of the applied voltage/current,[28,29] has also drawn considerable attention for the applications in nonvolatile memories, popularly known as ReRAM. Although there are few reports on the resistive switching behaviour of the $BiFeO_3$ thin films,[9,30] the same phenomenon for $BiFeO_3$ nanostructures still remains unexplored. The RS property of the $BiFeO_3/TiO_2$/Ti nano-heterostructures is shown in Figure 4(a). Inset of Figure 3(b) shows the schematic of the device where RS behaviour is recorded by applying a sweeping voltage as $-10\,V \rightarrow 0\,V \rightarrow +10\,V \rightarrow 0\,V \rightarrow -10\,V$ with Ti grounded at RT. A distinct non-volatile bipolar type anti-clockwise RS characteristics is observed (Figure 4(a)) without any "forming" process, and the device is found to repeat the same hysteresis behaviour even when the sweeping voltage is varied from $0\,V \rightarrow +10\,V \rightarrow 0\,V \rightarrow -10\,V \rightarrow 0\,V \rightarrow +10\,V$. During the voltage swept from 0 to $+10$ V, the resistance of the device is found to switch from a HRS to a LRS and a non-volatile "On" state was achieved. Figure 4(a) indicates that the current increased noticeably to a maximum value at around $+5$ V. The HRS and an "Off" state were achieved during the voltage sweep from 0 to -10 V. During the voltage swept from 0 to $+10$ V, the resistance varies from R_{Off} (HRS) $= 31 \times 10^9\,\Omega$ to R_{On} (LRS) $= 14 \times 10^9\,\Omega$ at round $+5$ V. The device is found to repeat the same stable hysteresis behaviour over time (Figure 4(b)). The device can be switched between HRS and LRS repeatedly a number of times, as shown in Figure 4(c) for the first five cycles. The intrinsic resistance memory effect of the device is evident from the reproducible *I–V* hysteresis.

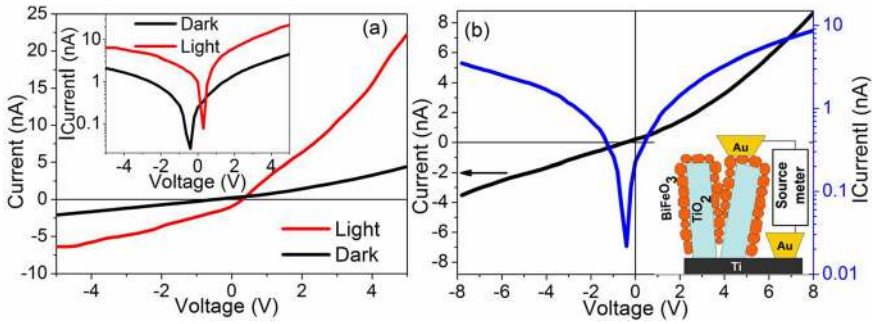

FIG. 3. (a) *I-V* curves of the $BiFeO_3/TiO_2$ nano-heterostructures under dark and light-illumination conditions. Inset of (a) shows the semi-log *I-V* curves of the $BiFeO_3/TiO_2$ nano-heterostructures. (b) *I-V* curves measured at a voltage range of ± 8 V on the $BiFeO_3/TiO_2$ nano-heterostructures under dark condition. Inset of (b) shows the sketch of the set up for the *I-V* measurements.

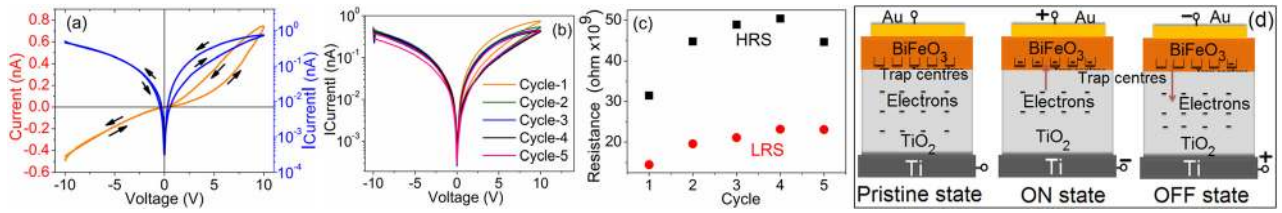

FIG. 4. (a) The *I-V* hysteresis curve indicating the RS behaviour for the $BiFeO_3/TiO_2/Ti$ nano-heterostructures. (b) The *I-V* hysteresis curves of the $BiFeO_3/TiO_2/Ti$ nano-heterostructures for the first five cycles. (c) Variation of LRS and HRS at +5 V over cycles. (d) Schematic illustration of the RS mechanism in $Au/BiFeO_3/TiO_2/Ti$ nano-heterostructures based on electron injection and trapping/detrapping process.

Generally, the RS behaviour of perovskite oxides is addressed based on two key mechanisms: conducting filament mechanism[1–4] and interface mechanism.[5–8] The filament type switching mechanism stands on the formation and rupture of local conductive filaments which results from the reorientation of oxygen vacancies[9,10] or the diffusion of metal ions.[11,12] On the other hand, the interface switching is demonstrated based on migration of oxygen vacancies[13] or interfacial carrier injection and trapping/detrapping process.[7,30–32] It is well known that both TiO_2 and $BiFeO_3$ are n-type semiconductors.[14] Here, the TiO_2 NTs contains large concentration of oxygen vacancies, as observed from XRD, XPS, and Raman studies (supplementary material),[15] which are known for the n-type characteristics of the TiO_2 and here the carrier (electrons) concentration in TiO_2 is higher than that of $BiFeO_3$. Furthermore, during the growth of $BiFeO_3$ on TiO_2 NTs by wet chemical route, a large number of interfacial defects appear in the nano-heterostructures. The formation of large concentration of defect states at the $BiFeO_3/TiO_2$ heterojunction is quite obvious because of the large surface areas of $BiFeO_3$ and TiO_2 nanostructures.[7] Now, these defect states can act as the "trapping centre," which can trap the migrating carriers (electrons) and control the electrical conductivity of the material significantly. The pristine state of the $BiFeO_3/TiO_2$ heterojunction is shown in Figure 4(d). Now, with the application of suitable negative bias on the Ti substrate, the electric field can force the migration of the electrons present in TiO_2 NTs across the $BiFeO_3/TiO_2$ hetero-interface to $BiFeO_3$ nanostructures. Thus, the applied electric field causes sudden increases of current, which results in LRS or "On" state.[7,30–32] The injected electrons across the $BiFeO_3/TiO_2$ hetero-interface get trapped at the trapping centres as shown in Figure 3(d).[7] The trapped electrons cannot be released until a large reverse voltage is applied to the device in the reset process, to overcome the built-in interfacial energy barrier, and thus the device achieves the "Off" state (HRS) in a reverse bias condition as shown in the schematic diagram in Figure 4(d). Therefore, it is expected that the injection/migration of the electrons from TiO_2 across the hetero-interface and the trapping/detrapping of the same at the defect/trapping centres present at the interface plays the key role in controlling the RS behaviour of the $BiFeO_3/TiO_2$ device. Moreover, $BiFeO_3$ being an electrochemically active material,[33] different ionic and electrochemical processes[34] also take place in the sample along with the above mentioned electronic process when the applied voltage is changed, leading to tuning the resistive switching property.

In summary, this study demonstrates the visible white-light tailored ferroelectricity, rectifying characteristics, photovoltaic effect, and the resistive switching behaviour of the $BiFeO_3$ nanostructures grown on insulating TiO_2 nanotube surface. The saturation ferroelectric polarization and remnant ferroelectric polarization are found to increase by 44% and 33%, respectively, at an external bias of 30 V after the irradiation of visible-light. The photo-ferroelectric response of the $BiFeO_3$ nanostructures becomes weaker with the increase of the applied external voltage. This external field-dependent photo-ferroelectric effect reveals that the trapping of the photo-generated electrons at the grain boundaries/interfaces controls the ferroelectric characteristics of $BiFeO_3$. $BiFeO_3/TiO_2$ nano-heterostructure also exhibits rectifying and photovoltaic characteristics along with the pronounced RS behaviour. RS mechanism of the device is demonstrated based on the field-induced injection/migration and trapped/detrapped process of electrons at the defect/trapping centres at the nano-interfaces. The $BiFeO_3/TiO_2$ nano-heterostructure device shows multifunctionality that integrates logic, memory, and photovoltaic properties.

Author Gobinda Gopal Khan is thankful to the Department of Science and Technology (DST), Government of India, for providing research support through the "INSPIRE Faculty Award" (IFA12-ENG-09). This work was supported by the start-up research grant (No. SB/FTP/ETA-0142/2014)

from Science and Engineering Research Board (SERB), Government of India.

[1]M. Fiebig, T. Lottermoser, D. Frohlich, A. V. Goltsev, and R. V. Pisarev, "Observation of coupled magnetic and electric domains," Nature **419**, 818–820 (2002).
[2]C. A. F. Vaz, J. Hoffman, C. H. Ahn, and R. Ramesh, "Magnetoelectric coupling effects in multiferroic complex oxide composite structures," Adv. Mater. **22**, 2900–2918 (2010).
[3]N. Hur, S. Park, P. A. Sharma, J. S. Ahn, S. Guha, and S. W. Cheong, "Electric polarization reversal and memory in a multiferroic material induced by magnetic fields," Nature **429**, 392–395 (2004).
[4]J. Wang, J. B. Neaton, H. Zheng, V. Nagarajan, S. B. Ogale, B. Liu, D. Viehland, V. Vaithyanathan, D. G. Schlom, U. V. Waghmare, N. A. Spaldin, K. M. Rabe, M. Wuttig, and R. Ramesh, "Epitaxial $BiFeO_3$ multiferroic thin film heterostructures," Science **299**, 1719–1722 (2003).
[5]M. Alexe and D. Hesse, "Tip-enhanced photovoltaic effects in bismuth ferrite," Nat. Commun. **2**, 256 (2011).
[6]T. Kimura, T. Goto, H. Shinatani, K. Ishizaka, T. Arima, and Y. Tokura, "Magnetic control of ferroelectric polarization," Nature **426**, 55–58 (2003).
[7]B. Sun, P. Han, W. Zhao, Y. Liu, and P. Chen, "White-light-controlled magnetic and ferroelectric properties in multiferroic $BiFeO_3$ square nanosheets," J. Phys. Chem. C **118**, 18814–18819 (2014).
[8]R. J. Zeches, M. D. Rossell, J. X. Zhang, A. J. Hatt, Q. He, C. H. Yang, A. Kumar, C. H. Wang, A. Melville, and C. A. Adamo, "Strain-driven morphotropic phase boundary in $BiFeO_3$," Science **326**, 977–980 (2009).
[9]T. Choi, S. Lee, Y. J. Choi, V. Kiryukhin, and S.-W. Cheong, "Switchable ferroelectric diode and photovoltaic effect in $BiFeO_3$," Science **324**, 63–66 (2009).
[10]C. Wang, K. J. Jin, Z. T. Xu, L. Wang, C. Ge, H. B. Lu, H. Z. Guo, M. He, and G. Z. Yang, "Switchable diode effect and ferroelectric resistive switching in epitaxial $BiFeO_3$ thin films," Appl. Phys. Lett. **98**, 192901 (2011).
[11]J. Kreisel, M. Alexe, and P. A. Thomas, "A photoferroelectric material is more than the sum of its parts," Nat. Mater. **11**, 260 (2012).
[12]Y. P. Wang, L. Zhou, M. F. Zhang, X. Y. Chen, J.-M. Liu, and Z. G. Liu, "Room-temperature saturated ferroelectric polarization in $BiFeO_3$ ceramics synthesized by rapid liquid phase sintering," Appl. Phys. Lett. **84**, 1731 (2004).
[13]K. Yin, M. Li, Y. Liu, C. He, F. Zhuge, B. Chen, W. Lu, X. Pan, and R.-W. Li, "Resistance switching in polycrystalline $BiFeO_3$ thin films," Appl. Phys. Lett. **97**, 042101 (2010).
[14]H. Yang, Y. Q. Wang, H. Wang, and Q. X. Jia, "Oxygen concentration and its effect on the leakage current in $BiFeO_3$ thin films," Appl. Phys. Lett. **96**, 012909 (2010).
[15]See supplementary material at http://dx.doi.org/10.1063/1.4940118 for the details of the fabrication and characterization of multifunctional $BiFeO_3$/TiO_2 nano-heterostructure.
[16]A. Sarkar, A. K. Singh, G. G. Khan, D. Sarkar, and K. Mandal, "TiO_2/ZnO core/shell nano-heterostructure arrays as photo-electrodes with enhanced visible light photoelectrochemical performance," RSC Adv. **4**, 55629–55634 (2014).
[17]R. Das, G. G. Khan, and K. Mandal, "Enhanced ferroelectric, magnetoelectric and magnetic properties in Pr and Cr co-doped $BiFeO_3$ nanotubes fabricated by template assisted route," J. Appl. Phys. **111**, 104115 (2012).
[18]T.-J. Park, G. C. Papaefthymiou, A. J. Viescas, A. R. Moodenbaugh, and S. S. Wong, "Size-dependent magnetic properties of single-crystalline multiferroic $BiFeO_3$ nanoparticles," Nano Lett. **7**, 766–772 (2007).
[19]V. M. Fridkin, *Photoferroelectrics* (Springer, 1979).
[20]A. L. Kholkin, S. O. Iakovlev, and J. L. Baptista, "Direct effect of illumination on ferroelectric properties of lead zirconate titanate thin films," Appl. Phys. Lett. **79**, 2055–2057 (2001).
[21]F. Rubio-Marcos, A. Del Campo, P. Marchet, and J. F. Ferna′ndez, "Ferroelectric domain wall motion induced by polarized light," Nat. Commun. **6**, 6594 (2015).
[22]D. Dimos, W. L. Warren, M. B. Sinclair, B. A. Tuttle, and R. W. Schwartz, "Photo induced hysteresis changes and optical storage in (Pb,La)(Zr,Ti)O_3 thin-films and ceramics," J. Appl. Phys. **76**, 4305–4315 (1994).
[23]W. Ji, K. Yao, and Y. C. Liang, "Bulk photovoltaic effect at visible wavelength in epitaxial ferroelectric $BiFeO_3$ thin films," Adv. Mater. **22**, 1763 (2010).
[24]F. Yan, G. Chen, L. Lu, and J. E. Spanier, "Dynamics of photogenerated surface charge on $BiFeO_3$ films," ACS Nano **6**, 2353–2360 (2012).
[25]D. Lee, S. H. Baek, T. H. Kim, J.-G. Yoon, C. M. Folkman, C. B. Eom, and T. W. Noh, "Polarity control of carrier injection at ferroelectric/metal interfaces for electrically switchable diode and photovoltaic effects," Phys. Rev. B **84**, 125305 (2011).
[26]Y. Cao, J. Shen, C. A. Randall, and L. Q. Chen, "Phase-field modeling of switchable diode-like current-voltage characteristics in ferroelectric $BaTiO_3$," Appl. Phys. Lett. **104**, 182905 (2014).
[27]C. Ge, K.-J. Jin, C. Wang, H.-B. Lu, C. Wang, and G.-Z. Yang, "Numerical investigation into the switchable diode effect in metal-ferroelectric-metal structures," Appl. Phys. Lett. **99**, 063509 (2011).
[28]K. Szot, W. Speier, G. Bihlmayer, and R. Waser, "Switching the electrical resistance of individual dislocations in single-crystalline $SrTiO_3$," Nat. Mater. **5**, 312–320 (2006).
[29]X. G. Chen, X. B. Ma, Y. B. Yang, L. P. Chen, G. C. Xiong, G. J. Lian, Y. C. Yang, and J. B. Yang, "Comprehensive study of the resistance switching in $SrTiO_3$ and Nb-doped $SrTiO_3$," Appl. Phys. Lett. **98**, 122102 (2011).
[30]Y. Zhu, M. Li, Z. Hu, X. Liu, Q. Wang, X. Fang, and K. Guo, "Nonvolatile resistive switching behaviour and the mechanism in Nd:$BiFeO_3$/Nb:$SrTiO_3$ heterostructure," J. Phys. D: Appl. Phys. **46**, 215305 (2013).
[31]X. Chen, G. Wu, H. Zhang, N. Qin, T. Wang, F. Wang, W. Shi, and D. Bao, "Nonvolatile bipolar resistance switching effects in multiferroic $BiFeO_3$ thin films on $LaNiO_3$ -electrodized Si substrates," Appl. Phys. A **100**, 987–990 (2010).
[32]K. M. Kim, B. J. Choi, M. H. Lee, G. H. Kim, S. J. Song, J. Y. Seok, J. H. Yoon, S. Han, and C. S. Hwang, "A detailed understanding of the electronic bipolar resistance switching behavior in Pt/TiO_2/Pt structure," Nanotechnology **22**, 254010 (2011).
[33]A. Sarkar, A. K. Singh, D. Sarkar, G. G. Khan, and K. Mandal, "Three-dimensional nanoarchitecture of $BiFeO_3$ anchored TiO_2 nanotube arrays for electrochemical energy storage and solar energy conversion," ACS Sustainable Chem. Eng. **3**, 2254–2263 (2015).
[34]E. Strelcov, Y. Kim, S. Jesse, Y. Cao, I. N. Ivanov, I. I. Kravchenko, C.-H. Wang, Y.-C. Teng, L.-Q. Chen, Y. H. Chu, and S. V. Kalinin, "Probing local ionic dynamics in functional oxides at the nanoscale," Nano Lett. **13**, 3455–3462 (2013).